Combining the individual effect of indicators to solve multi-objective optimization problems with different Pareto front geometries*

Jesús Guillermo Falcón-Cardona, Carlos A. Coello Coello and Michael T. M. Emmerich

CINVESTAV-IPN, Computer Science Department,
Av. IPN No. 2508, Col. San Pedro Zacatenco, México D.F. 07300, MEXICO
Leiden Institute of Advanced Computer Science, Leiden University,
Niels Bohrweg 1 2333 CA, Leiden, The Netherlands
jfalcon@computacion.cs.cinvestav.mx
ccoello@cs.cinvestav.mx
m.t.m.emmerich@liacs.leidenuniv.nl

Abstract. The use of multi-objective evolutionary algorithms (MOEAs) that employ a set of convex weight vectors as search directions, reference set or as part of a quality indicator has been widely extended. However, a recent study indicate that these MOEAs do not perform very well when tackling multi-objective optimization problem (MOPs), having different Pareto front geometries. Hence, it is necessary to propose MOEAs whose performance is not strongly correlated to specific Pareto front shapes. In this paper, we propose a MOEA that combines the individual effect of two indicator-based density estimators that do not employ convex weight vectors. The selected indicators are the IGD^+ and the s-energy which promote convergence and diversity of solutions, respectively. Our proposed approach, called CRS^+-EMOA, was compared with MOEAs using convex weight vectors (NSGA-III, MOEA/D and MOMBI2) and ones not using this set of vectors (Δ_p-MOEA and GDE-MOEA) on MOPs belonging to the test suites DTLZ, $DTLZ^{-1}$, WFG and WFG^{-1}. Experimental results show that CRS^+-EMOA outperforms the considered MOEAs, regarding the hypervolume and Solow-Polasky indicators, on most of the test problems and its performance does not depend on the Pareto front shape of the problems.

Keywords: Multi-Objective Optimization, Quality Indicators, Multi-Indicator Density Estimation

1 Introduction

In the last 30 years, Multi-Objective Evolutionary Algorithms (MOEAs), which are population-based and gradient-free metaheuristics, have arisen as a popu-

* The first author acknowledges support from CONACyT and CINVESTAV-IPN to pursue graduate studies in Computer Science. The second author gratefully acknowledges support from CONACyT project no. 221551.

lar approach to solve problems that involve the simultaneous optimization of several, often conflicting, objective functions [1].These problems are so-called multi-objective optimization problems (MOPs). MOEAs employ the principles of the natural evolution of individuals in order to drive a set of objective vectors towards the Pareto optimal front, that represent the solution to a MOP. In this regard, solving a MOP involves finding the best possible trade-offs among its objectives. The particular set that yields the optimum values is known as the Pareto Optimal Set ($\mathcal{P}^*$) and its image in objective space is known as the Pareto Optimal Front ($\mathcal{PF}^*$).

Currently, there are different design strategies of MOEAs, such as decomposition of the MOP into numerous single-objective optimization problems [2], the use of reference sets in order to attract the population towards the Pareto front [3], and the generation of selection mechanisms based on quality indicators[1] [4]. A wide variety of state-of-the-art MOEAs based on the strategies above mentioned commonly employ a set of convex weight vectors as search directions for the decomposition, in a method to construct reference sets, or as part of the definition of a quality indicator. A vector $\boldsymbol{w} \in \mathbb{R}^m$ is a convex weight vector if $\sum_{i=1}^{m} w_i = 1$ and $w_i \geq 0$ for all $i = 1, \ldots, m$. These weight vectors lie on an $(m-1)$-simplex. However, Ishibuchi *et al.* [5] empirically showed that the use of convex weight vectors overspecializes MOEAs on MOPs whose Pareto fronts are strongly correlated to the simplex formed by such weight vectors. In other words, such MOEAs are unable to produce good results when tackling MOPs whose Pareto fronts are not highly coupled with the $(m-1)$-simplex. In consequence, more general MOEAs need to be designed to avoid this overspecialization on specific benchmark problems such as the DTLZ and WFG test suites.

Other MOEAs do not use in any of their mechanisms a set of convex weight vectors. On the one hand, the Nondominated Sorting Genetic Algorithm II (NSGA-II) [6] uses Pareto dominance[2] in its main selection mechanism and crowding distance as the second selection mechanism. However, the selection pressure of NSGA-II dilutes when tackling MaOPs. Additionally, the crowding distance density estimator cannot produce evenly distributed Pareto fronts. On the other hand, the $\mathcal{S}$ Metric Selection Evolutionary Multi-Objective Algorithm (SMS-EMOA) [7] is a steady-state MOEA that replaces the crowding distance of NSGA-II by a density estimator based on the hypervolume indicator (HV) that measures convergence and distribution simultaneously. Although HV is the only unary Pareto-compliant[3] indicator, its use in MOEAs is prohibited since its computational cost exponentially increases as the number of objectives does. In

[1] A unary indicator I is a function that assigns a real value to set of points $\mathcal{A} = \{\boldsymbol{a}^1, \ldots, \boldsymbol{a}^N\}$, where $\boldsymbol{a}^i \in \mathbb{R}^m$.

[2] Given $\boldsymbol{u}, \boldsymbol{v} \in \mathbb{R}^m$, $\boldsymbol{u}$ Pareto dominates $\boldsymbol{v}$ (denoted as $\boldsymbol{u} \prec \boldsymbol{v}$) if and only if $\forall i = 1, \ldots, m, u_i \leq v_i$ and there exists at least an index $j \in \{1, \ldots, m\} : u_j < v_j$.

[3] Let $\mathcal{A}$ and $\mathcal{B}$ be two non-empty sets of m-dimensional vectors and let I be a unary indicator. I is Pareto-compliant if and only if $\mathcal{A}$ dominates $\mathcal{B}$ implies $I(\mathcal{A}) > I(\mathcal{B})$ (assuming maximization of I).

2015, Menchaca-Méndez and Coello proposed an environmental selection based on the Generational Distance (GD) indicator [8] coupled with a diversity mechanism that uses the ϵ dominance to divide the objective space into hypercubes where the solutions are distributed. A clear disadvantage of GDE-MOEA is the determination of the ϵ value in order to divide high-dimensional objective spaces which impact the generation of evenly distributed solutions. Finally, Δ_p-MOEA, proposed by Menchaca *et al.* [9], is an improvement of GDE-MOEA but instead of using GD in the selection mechanism, it uses the Δ_p indicator. Δ_p-MOEA improves the diversity of solutions, but it still depends on the calculation of the ϵ value to construct a reference set.

In order to overcome the above mentioned difficulties of MOEAs that do not use weight vectors, in this paper we propose an MOEA that takes advantage of the combination/synergy of the individual effect of two density estimators: one based on the IGD$^+$ indicator [10] and the other based on the s-energy indicator [11]. The main idea of our Evolutionary Multi-Objective Algorithm based on the Combination of the Riesz s-energy and IGD* (CRS$^+$-EMOA) is to analyze the convergence behavior during the search process statistically.. If the convergence behavior is stagnated, the generation of evenly distributed solutions is promoted using s-energy; otherwise, the IGD$^+$-based density estimator will drive the population to $\mathcal{PF}^*$.

The remainder of this paper is organized as follows. Section 2 gives some required definitions to the understanding of the paper. Our proposed approach is introduced in Sect. 3. The experimental results are discussed in Sect. 4. Finally, Section 5 outlines the main conclusions and future work.

2 Background

In this work, we focus, without loss of generality, on unconstrained MOPs that minimize all the objective functions. A MOP is formally defined as follows:

$$\min_{\boldsymbol{x}\in\Omega} \boldsymbol{F}(\boldsymbol{x}) = (f_1(\boldsymbol{x}), f_2(\boldsymbol{x}), \ldots, f_m(\boldsymbol{x}))^T, \tag{1}$$

where $\boldsymbol{x} \in \Omega \subseteq \mathbb{R}^n$ is the vector of decision variables and Ω is the decision variable space. $f_i : \mathbb{R}^n \to \mathbb{R}, i = 1, 2, \ldots, m$ are the objective functions, where $m \geq 2$. MOPs having four or more objective functions are called many-objective optimization problems (MaOPs).

In the following, two unary quality indicators are described. For this purpose, let $\mathcal{A}$ represent an approximation to $\mathcal{PF}^*$ and $\mathcal{Z} \subset \mathbb{R}^m$ be a reference set. On the one hand, Ishibuchi *et al.* proposed the Inverted Generational Distance plus (IGD$^+$) indicator in 2015 [10]. This indicator measures the average distance between $\mathcal{Z}$ and $\mathcal{A}$, using a modified Euclidean distance that takes into account Pareto dominance. Due to this modified distance, IGD$^+$ is a weakly Pareto compliant indicator. It is mathematically defined as follows:

$$\text{IGD}^+(\mathcal{A}, \mathcal{Z}) = \frac{1}{|\mathcal{Z}|} \sum_{\boldsymbol{z}\in\mathcal{Z}} \min_{\boldsymbol{a}\in\mathcal{A}} d^+(\boldsymbol{a}, \boldsymbol{z}), \tag{2}$$

where $d^+(\boldsymbol{a}, \boldsymbol{z}) = \sqrt{\sum_{k=1}^{m} \max(a_i - z_i, 0)^2}$ is the proposed modified Euclidean distance. On the other hand, Hardin and Saff proposed the s-energy indicator [11] in order to measure the even distribution of a set of points in k-dimensional manifolds. Its mathematical definition is given by the next formula:

$$E_s(\mathcal{A}) = \sum_{i \neq j} \|\boldsymbol{a}_i - \boldsymbol{a}_j\|^{-s} \tag{3}$$

where $s > 0$ is a fixed parameter that controls the grade of uniformity of the solutions in $\mathcal{A}$. Its minimization leads to evenly distributed solutions if $s \geq k$.

3 Our Proposed Approach

Quality indicators can be integrated into MOEAs in three different ways: 1) in the environmental selection mechanism, 2) as an update rule for archives, and 3) as density estimators (DEs). From these approaches, the latter has been widely used. An indicator-based density estimator (IB-DE) is the secondary selection mechanism of an MOEA. IB-DEs impose a total order among the solutions of an approximation set by calculating the individual contribution of each solution to the indicator value. Then, the worst-contributing solution is deleted from the population. In this work, we employed IGD^+ and s-energy as IB-DEs. Regarding IGD^+, the individual contribution C of a solution $\boldsymbol{a} \in \mathcal{A}$ is defined as follows: $C_{\text{IGD}^+}(\boldsymbol{a}, \mathcal{A}, \mathcal{Z}) = |\text{IGD}^+(\mathcal{A}, \mathcal{Z}) - \text{IGD}^+(\mathcal{A} \setminus \{\boldsymbol{a}\}, \mathcal{Z})|$. On the other hand, for s-energy, the individual contribution of $\boldsymbol{a} \in \mathcal{A}$ is given by: $C_{E_s}(\boldsymbol{a}, \mathcal{A}) = \frac{1}{2}[E_s(\mathcal{A}) - E_s(\mathcal{A} \setminus \{\boldsymbol{a}\})]$. On the basis of the above equations, IGD^+-DEs and E_s-DE are respectively defined as follows:

$$a_{\text{worst}} = \arg\min_{\boldsymbol{a} \in \mathcal{A}} C_{\text{IGD}^+}(\boldsymbol{a}, \mathcal{A}, \mathcal{Z}), \text{ and} \tag{4}$$

$$a_{\text{worst}} = \arg\max_{\boldsymbol{a} \in \mathcal{A}} C_{E_s}(\boldsymbol{a}, \mathcal{A}), \tag{5}$$

where a_{worst} denotes the wost-contributing value.

Algorithm 1 describes our proposed approach, called CRS^+-EMOA. CRS^+-EMOA is a steady-state MOEA that employs Pareto dominance in its environmental selection mechanism (using the nondominated sorting algorithm in line 6) and an IB-DE as secondary selection criterion. The main idea of CRS^+-EMOA is to exploit the properties of IGD^+ and s-energy by combining the individual effect of the corresponding IB-DEs. In other words, we want to drive the population towards the Pareto front using IGD^+-DE and, simultaneously, generating an evenly distributed approximation to the Pareto front through E_s-DE. To this end, CRS^+-EMOA switches between the two IB-DEs depending on a statistical analysis of the convergence behavior of the population, using an approximation to the hypervolume indicator (denoted as HV_{appr}). HV_{appr} is a simplification of the proposal of Ishibuchi *et al.* [12] and it sums up all the distances between an anti-optimal reference point $\boldsymbol{z}^{\max}$ and the set of current nondominated solutions

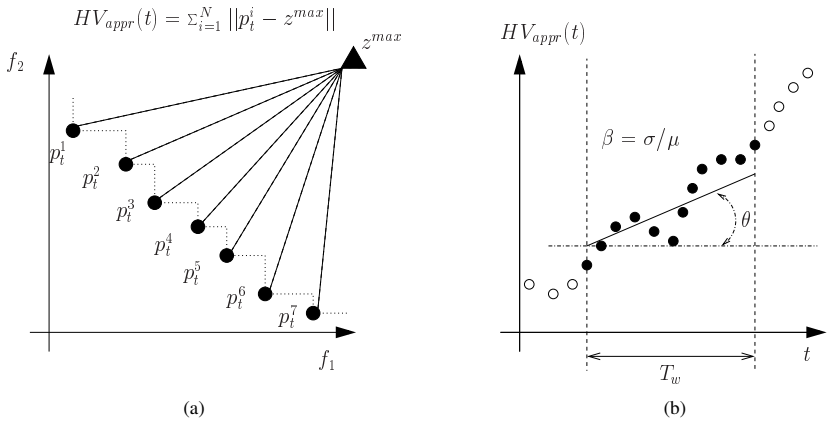

Fig. 1: (a) Hypervolume approximation sums up all the distances between the reference point and each nondominated solution, (b) linear model of the convergence behavior created using the last T_w measures of $\mathrm{HV}_{\mathrm{appr}}$.

(see Fig. 1a). At each iteration t, in line 7, $\boldsymbol{z}^{\max}$ is updated using the worst values of the current nondominated solutions and, then, $\mathrm{HV}_{\mathrm{appr}}(t)$ is computed such that the obtained value is stored in a circular array S_{HV} of size T_w. After the first T_w generations, S_{HV} will be full, and we can statistically analyze at each iteration the last T_w samples of $\mathrm{HV}_{\mathrm{appr}}$ as shown in Fig. 1b. In line 9, the mean μ and the standard deviation σ of the samples are computed such that the coefficient[4] of variation $\beta = \sigma/\mu$ is calculated. Additionally, the angle θ of a linear regression model of the samples is computed. Based on β and θ, we can exploit the properties of a certain IB-DE. If the number k of ranks produced by the nondominated sorting algorithm is equal to one and it holds that $\beta \leq \bar{\beta}$ and $\theta \in [-\bar{\theta}, \bar{\theta}]$ (where $\bar{\beta}$ and $\bar{\theta}$ are user-supplied parameters), it means that the convergence behavior is stagnated since there is not too much variation of $\mathrm{HV}_{\mathrm{appr}}$ and the linear model cannot be consider as ascending or descending. In consequence, we have to promote diversity using E_s-DE in line 11. Otherwise, if $L_k > 1$, IGD$^+$-DE is selected in line 14 in furtherance of improving the convergence of the population. In case $|L_k| = 1$, the sole individual in L_k is selected to elimination. Finally, the selected solution j_{worst} is deleted from the population, and a new generation is created.

[4] β is a standardized measure of dispersion that shows the extent of variability to the mean of the population.

Algorithm 1 CRS$^+$-EMOA general framework

Require: T_w, $\bar{\beta}$, $\bar{\theta}$
Ensure: Pareto front Approximation
Randomly initialize population P
$t \leftarrow 0$
while stopping criterion is not fulfilled **do**
  $q \leftarrow Variation(P)$
  $Q \leftarrow P \bigcup \{q\}$
  $\{L_1, L_2, \ldots, L_k\} \leftarrow$ nondominated-sorting(Q)
  Update reference point $\boldsymbol{z}^{\max}$ using L_1
  $S_{\text{HV}}[t \mod T_w] \leftarrow HV_{appr}(t)$
  Statistically analyze the last T_w samples in S_{HV} and generate β and θ
  if $k = 1$ and $\beta \leq \bar{\beta}$ and $\theta \in [-\bar{\theta}, \bar{\theta}]$ **then**
    $j_{\text{worst}} = \arg\max_{\boldsymbol{a} \in L_1} C_{E_s}(\boldsymbol{a}, L_1)$
  else
    if $|L_k| > 1$ **then**
      $j_{\text{worst}} = \arg\min_{\boldsymbol{a} \in L_k} C_{\text{IGD}^+}(\boldsymbol{a}, L_k, L_1)|$
    else
      j_{worst} is equal to the sole individual in L_k
  $P \leftarrow Q \setminus \{j_{\text{worst}}\}$
  $t \leftarrow t + 1$
return P

4 Experimental Results

In this section, we analyze the performance of CRS$^+$EMOA[5] in comparison with different state-of-the-art MOEAs, namely NSGA-III [3], MOEA/D [2], MOMBI2 [4], Δ_p-MOEA [9] and GDE-MOEA [8]. The adopted MOEAs are classified into two main groups: MOEAs based on convex weight vectors and MOEAs not using convex weight vectors. NSGA-III[6], MOEA/D[7] and MOMBI2[8] belong to the first group while the remaining MOEAs[9] belong to the other group. We adopted MOPs of the benchmarks DTLZ and WFG [13], as well as from the minus versions of them denoted as DTLZ^{-1} and WFG^{-1} that were proposed by Ishibuchi *et al.* [5]. The use of the minus versions of the benchmarks is to determine the performance of the considered MOEAs on MOPs whose Pareto fronts are not correlated to the simplex formed by a set of convex weight vectors. Additionally,

[5] The source code of CRS$^+$-EMOA is available at `http://computacion.cs.cinvestav.mx/~jfalcon/CRS.html`.
[6] We used the implementation available at: `http://web.ntnu.edu.tw/~tcchiang/publications/nsga3cpp/nsga3cpp.htm`.
[7] We used the implementation available at: `http://dces.essex.ac.uk/staff/zhang/webofmoead.htm`.
[8] We used the implementation available at `http://computacion.cs.cinvestav.mx/~rhernandez/`.
[9] The source code of Δ_p-MOEA and GDE-MOEA was provided by its author Adriana Menchaca Méndez.

the Pareto fronts of these MOPs cover a wide range of geometries such as linear, concave, degenerated, disconnected and mixed. In each case, we employed 3, 5 and 10 objective functions. In order to measure the performance of CRS$^+$-EMOA and the adopted MOEAs, we applied the hypervolume and the Solow-Polasky indicators [14] for measuring convergence and diversity, respectively. For each MOEA in each test instance, we performed 30 independent executions.

4.1 Parameters settings

Table 1: Parameters adopted in our experiments.

Objectives (m)		3	5	7	10
Population size		120	126	210	220
Objective function evaluations ($\times 10^3$)		50	70	90	120
WFG	variables (n)	26	30	34	40
WFG	position-related parameters	2	4	6	9
Weight-vector partitions (H)		14	5	4	3

Since our approach and all the considered MOEAs are genetic algorithms that use Simulated Binay Crossover and Polynomial Mutation as variation operators, we set the crossover probability (P_c), crossover distribution index (N_c), mutation probability (P_m), and the mutation distribution index (N_m) as follows. For MOPs having three objective functions $P_c = 0.9$ and $N_c = 20$, while for MaOPs $P_c = 1.0$ and $N_c = 30$. In all cases, $P_m = 1/n$, where n is the number of decision variables, and $N_m = 20$. Table 1 shows the population size N, objective function evaluations (employed as the stopping criterion) and the parameter H for the generation of the set of convex weight vectors.It is worth noting that we set $N = C_{m-1}^{H+m-1}$. Table 1 also describes the number of variables and position-related parameters employed for the WFG and WFG^{-1} problems. Considering the DTLZ and DTLZ^{-1} instances, the number of variables is equal to $n = m + K - 1$, where $K = 5$ for DTLZ1 and DTLZ1^{-1}, $K = 10$ for DTLZ2, DTLZ5 and their minus versions, and $K = 20$ for DTLZ7 and DTLZ7^{-1}. For MOEA/D, the neighborhood size was set to 20 in all cases. Regarding CRS$^+$-EMOA, we employed $T_w = N$, $\bar{\beta} = 0.1$ and $\bar{\theta} = 0.25$ degrees for all instances.

4.2 Discussion of results

Tables 2 and 3 show the mean and standard deviation (in parentheses) obtained by all the compared algorithms for the hypervolume and Solow-Polasky indicators, respectively. The two best values among the MOEAs are emphasized in grayscale, where the darker tone corresponds to the best value. Aiming to have

the statistical confidence in the results, we performed a one-tailed Wilcoxon test using a significance level of 0.05. Based on the Wilcoxon test, the symbol # is placed when CRS$^+$-EMOA performs better than other MOEA in a statistically significant way.

Regarding the hypervolume indicator, CRS$^+$-EMOA is the best algorithm since it obtained the first place in 50% of the test problems. The second place corresponds to NSGA-III because it is the best MOEA in 8 out of 42 problems. However, it is worth emphasizing that for the minus benchmarks, NSGA-III only obtained one first place, specifically for DTLZ7^{-1} in 3 objective functions. In this regard, MOEA/D and MOMBI2 have just one first place in these minus benchmarks, and the remaining of their first places belong to the original DTLZ and WFG test suites. In consequence, it is clear the overspecialization of MOEAs using convex weight vectors on these benchmarks. Considering Δ_p-MOEA and GDE-MOEA, their performance is not so high. In fact, GDE-MOEA never obtains the first place and Δ_p-MOEA is the best algorithm in four test instances.

The Solow-Polasky indicator supports the good results of CRS$^+$-EMOA. This indicator measures the number of species present in the population. Thus, a larger value of the indicator is better because it means a good diversity of solutions. Our proposed approach produces well-distributed Pareto fronts in 26 out of 42 test instances (see Fig. 2). As a matter of fact, in most of the cases when CRS$^+$-EMOA obtains the best HV value, it also obtains the best Solow-Polasky value. Hence, this a first insight that the synergy between IGD$^+$ and s-energy is actually responsible of its good performance in both convergence and diversity. Regarding the other MOEAs, NSGA-III and Δ_p-MOEA tie in second place since they obtained the best indicator value in 5 problems. Once again, NSGA-III can only produce good results for the original DTLZ and WFG problems. The worst algorithm regarding this indicator is related to MOMBI2.

For DTLZ1 and DTLZ1^{-1} that have a linear Pareto front, CRS$^+$-EMOA does not obtain the best HV value. However, the Solow-Polasky indicator demonstrates that our approach has a better diversity. The top part of Fig. 2 shows the DTLZ1^{-1} fronts produced by all MOEAs, and it is evident that CRS$^+$-EMOA produces an evenly distributed front in comparison with the adopted MOEAs. MOEA/D and MOMBI2 generate numerous solutions in the boundary of the front, while Δ_p-MOEA, GDE-MOEA and NSGA-III do not produce well-distributed solutions. For convex problems, i.e., DTLZ2^{-1} and DTLZ5^{-1}, it is evident that CRS$^+$-EMOA has a good performance. This is because it entirely covers the Pareto front, unlike the other MOEAs that do not. This effect is illustrated in the second row of Fig. 2. For more complicated problems such as DTLZ7 and WFG2^{-1} that prove the ability of MOEA to manage subpopulations, it is evident from the Figure that CRS$^+$-MOEA produces better results. In the light of these results, we can claim that CRS$^+$-EMOA is a more general optimizer because its performance is not strongly linked to certain types of benchmark problems.

Table 2: Mean and standard deviation (in parentheses) of the Hypervolume indicator. A symbol # is placed when CRS$^+$-EMOA performed significantly better than the other approaches based on a one-tailed Wilcoxon test using a significance level of $\alpha = 0.05$. The two best values are shown in gray scale, where the darker tone corresponds to the best value.

Problema	Dim.	CRS$^+$-EMOA	NSGA-III	MOEA/D	MOMBI2	Δ_p-MOEA	GDE-MOEA
DTLZ1	3	9.739039e-01 (3.858675e-04)	9.741141e-01 (3.120293e-04)	9.740945e-01 (2.619649e-04)	9.663444e-01# (1.080932e-03)	9.413310e-01# (1.964370e-02)	9.676446e-01# (2.362618e-03)
	5	9.877798e-01 (3.117917e-03)	9.986867e-01 (3.379577e-05)	9.986355e-01 (3.735697e-05)	9.904662e-01 (1.120127e-03)	3.320501e-02# (8.565974e-02)	4.840903e-01# (4.857106e-01)
	10	9.963635e-01 (1.065991e-03)	9.999939e-01 (2.139857e-06)	9.996746e-01 (1.025281e-04)	9.961538e-01 (9.574496e-04)	3.040882e-02# (5.310077e-02)	0.000000e+00# (0.000000e+00)
DTLZ2	3	7.419537e+00 (3.056980e-03)	7.421572e+00 (6.064709e-04)	7.421715e+00 (1.372809e-04)	7.380040e+00# (7.076656e-03)	7.371981e+00# (3.875638e-02)	7.350569e+00# (2.220661e-02)
	5	3.157090e+01 (2.415933e-02)	3.166721e+01 (6.548007e-04)	3.166781e+01 (5.129480e-04)	3.149886e+01# (2.619865e-02)	3.145814e+01# (6.277721e-02)	3.139858e+01# (7.085084e-02)
	10	1.021699e+03 (4.906893e-01)	1.023905e+03 (1.423610e-03)	1.023902e+03 (4.192719e-03)	1.022163e+03 (4.299615e-01)	1.022172e+03 (3.206973e-01)	8.223136e+02# (4.847301e+01)
DTLZ5	3	6.103498e+00 (2.913259e-04)	6.086240e+00# (3.462620e-03)	6.046024e+00# (2.227008e-04)	6.018466e+00# (3.166178e-03)	6.083103e+00# (4.024434e-02)	6.070736e+00# (4.307412e-02)
	5	2.306362e+01 (2.295313e-01)	2.162912e+01# (9.476133e-01)	2.328373e+01 (1.640165e-02)	2.175597e+01# (2.378197e-01)	2.152316e+01# (1.422545e+00)	1.943602e+01# (1.234198e+00)
	10	6.453781e+02 (4.080592e+01)	6.172582e+02# (4.132326e+01)	7.043390e+02 (1.714256e+00)	6.054385e+02# (4.091687e+01)	5.909772e+02# (7.644220e+01)	9.641241e+01# (1.554238e+01)
DTLZ7	3	1.634605e+01 (5.285233e-02)	1.631926e+01# (1.253568e-02)	1.620770e+01# (1.240925e-01)	1.613885e+01# (3.101462e-02)	1.612577e+01# (1.553168e-01)	1.615480e+01# (1.492618e-01)
	5	1.281085e+01 (1.974810e-01)	1.284401e+01 (3.182259e-02)	6.515913e+00# (1.170945e+00)	1.269646e+01# (4.907749e-02)	1.255217e+01# (1.341411e-01)	1.234590e+01# (2.234605e-01)
	10	3.479852e+00 (2.403388e-01)	1.806637e+00# (4.781492e-01)	2.756082e-03# (7.839814e-03)	3.033892e+00# (5.070947e-02)	3.027342e+00# (9.110566e-02)	2.080502e+00# (4.312007e-01)
WFG1	3	5.056544e+01 (1.657420e+00)	4.917540e+01# (1.742752e+00)	4.994533e+01 (2.615320e+00)	5.250059e+01 (1.702362e+00)	3.624458e+01# (9.571499e-01)	3.857628e+01# (9.613983e-01)
	5	4.509188e+03 (1.444159e+02)	4.049661e+03# (1.445036e+02)	4.522924e+03 (1.145447e+02)	4.682300e+03 (7.687667e+01)	3.198417e+03# (8.802857e+01)	3.499936e+03# (7.077142e+01)
	10	5.037589e+09 (8.535179e+07)	4.333786e+09# (4.767509e+07)	4.626119e+09# (9.082857e+07)	5.028893e+09 (6.062765e+07)	3.422833e+09# (2.182108e+07)	3.554077e+09# (4.491835e+07)
WFG2	3	1.000262e+02 (2.196919e-01)	1.000303e+02 (2.020421e-01)	9.425491e+01# (1.887090e+00)	9.995196e+01# (2.218338e-01)	2.860787e+01# (1.562061e-01)	2.878405e+01# (3.147546e-02)
	5	1.008420e+04 (5.737764e+01)	1.022660e+04 (2.444328e+01)	9.147103e+03# (2.989196e+02)	1.021265e+04 (2.425440e+01)	2.356563e+03# (1.302041e+01)	2.352252e+03# (2.298487e+01)
	10	1.348499e+10 (4.708062e+07)	1.343510e+10# (5.838755e+07)	1.153362e+10# (4.307707e+08)	1.346239e+10 (6.456777e+07)	2.433110e+09# (1.405830e+07)	2.417620e+09# (3.423298e+07)
WFG3	3	7.306197e+01 (3.258533e-01)	7.359113e+01 (3.698540e-01)	6.949014e+01 (2.043137e+00)	7.476737e+01 (2.010304e-01)	2.974536e+01 (2.198130e-01)	3.026476e+01 (9.539859e-02)
	5	6.735962e+03 (9.568603e+01)	6.705622e+03 (6.623165e+01)	5.831355e+03# (1.740491e+02)	6.720322e+03 (8.790247e+01)	2.425136e+03# (2.737458e+01)	2.467475e+03# (5.330311e+00)
	10	8.262095e+09 (2.467236e+08)	7.851751e+09# (1.420734e+08)	3.407782e+09# (4.406816e+08)	7.150575e+09# (8.942471e+08)	2.435088e+09# (7.572200e+07)	2.460728e+09# (2.651078e+07)
DTLZ1^{-1}	3	2.237019e+07 (1.096230e+05)	2.044422e+07# (2.230718e+05)	1.708422e+07# (2.776295e+05)	1.754720e+07# (1.024912e+04)	2.249206e+07 (9.308520e+04)	2.178413e+07# (1.919526e+05)
	5	5.990400e+10 (5.969126e+09)	1.653440e+10# (7.395153e+09)	1.275157e+10# (5.929635e+09)	1.829497e+10# (1.178680e+08)	8.421535e+10 (5.019922e+09)	7.834908e+10 (5.592427e+09)
	10	2.331601e+15 (1.332180e+15)	1.690928e+16 (1.594681e+16)	2.068669e+10# (2.776909e+10)	3.254959e+17 (7.964585e+16)	4.163772e+17 (1.784438e+17)	1.959914e+17 (7.692566e+16)
DTLZ2^{-1}	3	1.255756e+02 (1.372903e-01)	1.226427e+02# (4.332124e-01)	1.241646e+02# (1.767939e-01)	1.246298e+02# (1.975120e-02)	1.202429e+02# (1.235826e+00)	1.232392e+02# (4.384877e-01)
	5	1.823404e+03 (5.652832e+00)	1.529187e+03# (3.829295e+01)	1.570781e+03# (5.466206e+00)	1.377041e+03# (2.801096e+00)	1.615070e+03# (3.622796e+01)	1.684100e+03# (2.422012e+01)
	10	3.952305e+05 (6.000728e+03)	2.480210e+05# (3.215706e+04)	1.837497e+05# (3.540744e+03)	1.941735e+05# (4.318334e+03)	4.467775e+05 (1.153133e+04)	4.295481e+05 (1.104582e+04)
DTLZ5^{-1}	3	1.240446e+02 (1.543643e-01)	1.212729e+02# (4.506920e-01)	1.230132e+02# (1.173182e-01)	1.233805e+02# (2.897257e-02)	1.191790e+02# (1.218659e+00)	1.217996e+02# (3.913095e-01)
	5	1.830136e+03 (8.376583e+00)	1.526551e+03# (4.186892e+01)	1.532378e+03# (6.612506e+00)	1.490703e+03# (3.599646e+00)	1.550531e+03# (3.545733e+01)	1.663295e+03# (2.143198e+01)
	10	5.043244e+05 (5.933536e+03)	2.353908e+05# (2.658733e+04)	1.618586e+05# (2.870596e+03)	1.786897e+05# (4.650613e+03)	3.841427e+05# (1.267929e+04)	3.788162e+05# (1.409232e+04)
DTLZ7^{-1}	3	2.139263e+02 (1.705184e+00)	2.144482e+02 (1.844494e-02)	2.144785e+02 (3.401603e-03)	2.144350e+02 (1.484695e-02)	2.141398e+02 (6.446048e-01)	2.117720e+02# (5.620357e+00)
	5	1.193104e+03 (7.463449e+00)	1.190442e+03# (4.159670e+00)	6.388549e+02# (5.254422e+01)	1.197724e+03 (5.760920e+00)	1.195714e+03 (1.560565e+00)	1.167397e+03# (3.067229e+01)
	10	6.493424e+04 (1.799575e+02)	6.282093e+04# (1.236603e+02)	7.555843e+03# (6.397426e+02)	6.278498e+04# (5.606912e+02)	6.374490e+04# (1.597907e+02)	6.336153e+04# (1.579373e+02)
WFG1^{-1}	3	4.721465e+02 (5.118363e+01)	5.214593e+02 (2.613138e+01)	3.653092e+02# (2.305800e+00)	4.717969e+02# (4.848793e+01)	4.289752e+02# (4.089696e+01)	4.226979e+02# (4.328855e+01)
	5	8.957760e+04 (1.295509e+04)	6.766707e+04# (3.634016e+03)	4.312409e+04# (1.486578e+03)	8.604789e+04 (1.028243e+04)	6.687040e+04# (8.125469e+03)	5.398842e+04# (6.022448e+03)
	10	1.920711e+11 (1.254828e+10)	1.167307e+11# (9.811376e+09)	7.403214e+10# (3.748511e+09)	5.753336e+10# (1.586430e+09)	1.037099e+11# (5.197695e+09)	8.712812e+10# (9.507560e+09)
WFG2^{-1}	3	7.318853e+02 (4.584376e-01)	7.256549e+02# (2.471515e+00)	7.318071e+02# (5.137348e-01)	7.277336e+02# (7.218694e-01)	3.548073e+02# (4.631427e-01)	3.549143e+02# (1.951948e-01)
	5	1.638383e+05 (1.165835e+03)	1.470928e+05# (8.586496e+03)	1.122933e+05# (1.197256e+04)	1.499384e+05# (4.291788e+02)	4.315723e+04# (1.487567e+02)	4.156049e+04# (6.526206e+02)
	10	7.365072e+11 (6.254171e+09)	3.658776e+11# (1.973606e+10)	2.462168e+11# (2.934157e+10)	8.919695e+10# (1.091716e+10)	7.359311e+10# (2.277690e+08)	7.165991e+10# (8.580112e+08)
WFG3^{-1}	3	6.701244e+02 (9.728569e-01)	6.581207e+02# (2.461272e+00)	6.559404e+02# (1.399701e-01)	6.678986e+02# (4.368737e-01)	3.901185e+02# (2.837691e+00)	3.929122e+02# (1.663457e+00)
	5	1.460039e+05 (2.618698e+03)	1.271888e+05# (5.065268e+03)	9.818104e+04# (4.519958e+03)	1.345863e+05# (2.667741e+02)	4.822825e+04# (1.017141e+03)	4.912237e+04# (6.555485e+02)
	10	6.613123e+11 (2.015972e+10)	3.003925e+11# (2.070638e+10)	1.932277e+11# (2.123809e+10)	1.572410e+11# (3.994016e+09)	8.120430e+10# (2.177319e+09)	8.405921e+10# (1.518237e+09)

Table 3: Mean and standard deviation (in parentheses) of the Solow-Polasky indicator. A symbol # is placed when CRS$^+$-EMOA performed significantly better than the other approaches based on a one-tailed Wilcoxon test using a significance level of $\alpha = 0.05$. The two best values are shown in gray scale, where the darker tone corresponds to the best value.

Problema	Dim.	CRS$^+$-EMOA	NSGA-III	MOEA/D	MOMBI2	Δ_p-MOEA	GDE-MOEA
DTLZ1	3	9.944608e+00 (7.332450e-01)	9.394548e+00# (2.930251e-01)	9.314418e+00# (3.914884e-02)	9.000566e+00# (2.446366e-02)	7.811889e+00# (9.608413e-01)	9.208526e+00# (7.142910e-01)
	5	1.338590e+01 (5.394744e-01)	1.927839e+01 (2.200570e-01)	1.910784e+01 (2.012103e-01)	1.784107e+01 (5.535436e-02)	1.258001e+02 (3.614573e-01)	7.251588e+01 (4.806114e+01)
	10	1.785253e+01 (8.881198e-01)	4.215677e+01 (2.267717e+00)	3.557264e+01 (6.064497e-01)	3.493408e+01 (2.073537e+00)	2.196627e+02 (4.229255e-01)	1.937667e+02 (5.463117e+00)
DTLZ2	3	3.395527e+01 (9.380927e-02)	3.394704e+01# (1.377030e-02)	3.393654e+01# (1.057577e-03)	3.320388e+01# (3.200128e-02)	3.071966e+01# (5.648283e-01)	3.130480e+01# (3.907121e-01)
	5	9.880242e+01 (3.075202e+00)	1.023559e+02 (2.316020e-01)	1.017397e+02 (4.330518e-03)	1.000214e+02 (9.376416e-02)	9.047203e+01# (1.071667e+00)	8.885177e+01# (1.407456e+00)
	10	2.144437e+02 (8.333968e-01)	2.144143e+02# (4.461039e-02)	2.140218e+02# (1.052798e-02)	2.134074e+02# (2.440550e-01)	2.073661e+02# (1.076644e+00)	2.149790e+02 (1.820800e+00)
DTLZ5	3	8.835302e+00 (8.683488e-03)	8.689954e+00# (4.814112e-02)	4.565503e+01 (6.372947e-01)	8.446415e+00# (1.275105e-02)	8.725615e+00# (1.118233e-01)	9.131640e+00 (8.893988e-01)
	5	5.453458e+01 (3.836635e+00)	7.846618e+01 (3.806546e+00)	2.193721e+01# (7.192604e-01)	1.733111e+01# (1.215347e+00)	6.458870e+01 (4.414063e+00)	9.229364e+01 (3.153601e+00)
	10	1.426916e+02 (1.105651e+01)	1.855864e+02 (4.441145e+00)	7.636613e+00# (7.127440e-02)	2.097795e+01# (1.446842e+01)	1.636387e+02 (1.190412e+01)	2.009986e+02 (2.726407e+00)
DTLZ7	3	4.693189e+01 (4.563587e+00)	4.248938e+01# (8.838503e-01)	3.411613e+01# (6.885687e+00)	3.750968e+01# (4.295088e-01)	3.356066e+01# (8.918332e+00)	3.791999e+01# (1.074318e+01)
	5	7.703740e+01 (2.640331e+01)	9.605921e+01 (4.006295e+00)	2.595428e+01# (3.104755e-01)	7.335971e+01# (1.892378e+00)	1.014229e+02 (7.384253e+00)	8.467007e+01 (2.946531e+01)
	10	2.083721e+02 (1.401193e+01)	3.401405e+01# (4.627073e+01)	6.635493e+00# (8.377910e-01)	1.539631e+02# (1.794040e+01)	2.161036e+02 (1.887145e+00)	1.635677e+02# (5.659825e+01)
WFG1	3	6.266729e+01 (4.306665e+00)	5.624993e+01# (4.311929e+00)	5.053063e+01# (2.764405e+00)	5.406056e+01# (2.296813e+00)	3.936107e+01# (2.712236e+00)	4.901870e+01# (2.752851e+00)
	5	7.766310e+01 (9.797998e+00)	9.244372e+01 (7.266040e+00)	7.480740e+01 (3.832994e+00)	7.292172e+01# (5.425443e+00)	5.404634e+01# (4.708150e+00)	9.197836e+01 (4.116442e+00)
	10	1.153389e+02 (1.285140e+01)	8.917693e+01# (8.545945e+00)	1.552376e+01# (3.169355e+00)	6.819405e+01# (8.992674e+00)	9.420152e+01# (6.434297e+00)	1.681839e+02 (7.642626e+00)
WFG2	3	1.031961e+02 (6.913412e-01)	9.475339e+01# (5.942618e-01)	7.243218e+01# (1.099197e+00)	8.113447e+01# (1.694539e+00)	1.566893e+01# (4.695226e-01)	1.597100e+01# (5.210876e-01)
	5	9.923778e+01 (3.753788e+00)	1.259866e+02 (5.442239e-01)	9.750359e+01# (2.449040e+00)	1.226234e+02 (1.081329e+00)	2.491924e+01# (1.910851e+00)	2.346945e+01# (2.689896e+00)
	10	1.981494e+02 (4.297874e+00)	2.034942e+02 (6.167357e+00)	2.746068e+01# (9.314055e+00)	1.826284e+02# (2.286544e+01)	5.897645e+01# (4.305811e+00)	5.040485e+01# (7.890364e+00)
WFG3	3	7.979549e+01 (8.271398e-01)	5.447458e+01# (3.954759e+00)	6.745390e+01# (1.429561e+00)	4.359786e+01# (9.246690e-01)	2.088260e+01# (5.548807e-01)	2.237972e+01# (2.670741e-01)
	5	1.207901e+02 (1.514908e+00)	9.114798e+01# (4.803291e+00)	1.203892e+02# (1.120195e+00)	3.884532e+01# (5.191645e+00)	3.640185e+01# (1.590306e+00)	3.986356e+01# (1.669298e+00)
	10	2.198151e+02 (1.511883e-01)	1.842494e+02# (6.381996e+00)	1.685512e+02# (8.180955e-01)	1.223302e+02# (2.606946e+01)	7.655449e+01# (7.601122e+00)	9.569073e+01# (5.324356e+00)
DTLZ1^{-1}	3	1.238722e+02 (6.478345e-01)	1.192301e+02# (9.769981e-01)	1.110656e+02# (2.067972e-01)	1.076858e+02# (1.612270e+00)	1.194494e+02# (7.076038e-01)	1.026058e+02# (2.385964e+00)
	5	1.261138e+02 (3.746123e-01)	1.276049e+02 (7.483806e-01)	1.160278e+02# (3.018754e+00)	6.760143e+01# (4.891955e+00)	1.256546e+02# (4.961652e-01)	1.091644e+02# (2.978643e+00)
	10	2.200000e+02 (6.478398e-01)	2.194982e+02# (5.550208e-01)	1.845834e+01# (3.362045e+01)	2.177230e+02# (1.598879e+00)	2.199297e+02# (1.852502e-01)	1.956693e+02# (3.843626e+00)
DTLZ2^{-1}	3	1.129425e+02 (2.079720e-01)	9.168006e+01# (2.394444e+00)	9.466441e+01# (8.426911e-02)	9.433643e+01# (1.896075e-01)	8.857439e+01# (2.604729e+00)	8.818635e+01# (2.087133e+00)
	5	1.259981e+02 (4.099458e-04)	1.134723e+02# (2.970256e+00)	1.247875e+02# (1.631879e-01)	4.888021e+01# (1.111632e+00)	1.185054e+02# (1.679308e+00)	1.078721e+02# (2.347639e+00)
	10	2.249876e+02 (1.368722e+00)	2.075064e+02# (3.824826e+00)	2.079851e+02# (1.899257e+00)	1.810577e+02# (3.309000e+00)	2.118042e+02# (2.291510e+00)	1.931317e+02# (4.552358e+00)
DTLZ5^{-1}	3	1.069995e+02 (2.945855e-01)	8.469885e+01# (1.989703e+00)	7.942908e+01# (2.711812e-01)	8.622124e+01# (1.733700e-01)	8.484735e+01# (2.558670e+00)	8.305258e+01# (1.583665e+00)
	5	1.259747e+02 (3.780629e-03)	1.041424e+02# (3.722763e+00)	1.229014e+02# (1.837627e-01)	4.957223e+01# (1.976910e+00)	1.180479e+02# (1.846989e+00)	1.076183e+02# (2.710724e+00)
	10	2.199997e+02 (6.289321e-05)	1.579241e+02# (1.854156e+01)	1.997485e+02# (1.822188e+00)	1.636386e+02# (7.545337e+00)	2.094613e+02# (2.217251e+00)	1.946215e+02# (3.565477e+00)
DTLZ7^{-1}	3	2.345500e+01 (6.661044e+00)	2.375280e+01 (1.117994e+00)	2.588876e+01 (3.461387e+00)	1.994117e+01# (4.519640e-01)	2.178525e+01# (8.341601e-01)	1.805087e+01# (8.596927e+00)
	5	5.660901e+01 (1.568211e+01)	7.238636e+01 (1.269825e+01)	1.211841e+01# (1.172186e+00)	4.067053e+01# (9.192226e+00)	8.003609e+01 (3.156330e+00)	3.632242e+01# (3.834467e+01)
	10	2.043557e+02 (1.375176e+01)	1.347251e+01# (4.083423e+00)	4.293619e+00# (1.198274e-01)	8.812385e+00# (2.123041e+01)	2.008713e+02# (2.214667e+00)	2.028099e+02# (5.987172e+00)
WFG1^{-1}	3	6.415681e+01 (4.459890e+00)	5.511082e+01# (2.648385e+00)	1.663876e+01# (1.535080e+00)	4.730483e+01# (1.092483e+00)	4.842279e+01# (5.020350e+00)	4.279700e+01# (1.538301e+01)
	5	1.210334e+02 (2.192520e+00)	5.596308e+01# (5.654765e+00)	7.815456e+00# (1.225035e+00)	3.289189e+01# (2.858823e+00)	1.098994e+02# (4.122587e+00)	5.939438e+01# (3.673750e+01)
	10	2.186105e+02 (3.132639e-01)	6.927501e+01# (2.258115e+01)	2.480353e+00# (2.063527e+00)	3.476224e+01# (4.296041e+00)	1.950445e+02# (6.121614e+00)	1.138247e+02# (5.884228e+01)
WFG2^{-1}	3	1.140860e+02 (4.325357e-01)	9.532850e+01# (1.992380e+00)	8.890140e+01# (1.794800e-01)	9.018353e+01# (4.679018e-01)	3.230763e+00# (4.485117e-02)	2.757698e+00# (2.020626e-01)
	5	1.234346e+02 (7.027142e-01)	9.827363e+01# (2.826007e+00)	4.956629e+01# (8.529213e+00)	3.689443e+01# (1.559225e+00)	5.922537e+00# (7.879377e-01)	2.841850e+00# (6.498607e-01)
	10	2.196197e+02 (9.739353e-02)	2.001692e+02# (4.030917e+00)	2.500717e+01# (2.754994e+00)	1.075588e+02# (1.284360e+01)	1.138578e+01# (8.309404e-01)	7.783812e+00# (1.059255e+00)
WFG3^{-1}	3	1.075596e+02 (2.777510e-01)	7.484580e+01# (2.494935e+00)	6.164392e+01# (7.387154e-02)	7.097018e+01# (1.699291e-01)	2.303097e+01# (7.406376e-01)	2.381595e+01# (2.661523e-01)
	5	1.259055e+02 (2.786019e-02)	8.633630e+01# (4.246132e+00)	6.654930e+01# (3.739241e+00)	3.937358e+01# (1.177063e+00)	3.626087e+01# (2.423541e+00)	4.063424e+01# (2.006301e+00)
	10	2.199995e+02 (8.710466e-04)	1.929382e+02# (8.857025e+00)	5.251797e+01# (3.065445e+00)	1.414077e+02# (1.791224e+01)	7.135125e+01# (7.053632e+00)	9.336338e+01 (4.573319e+00)

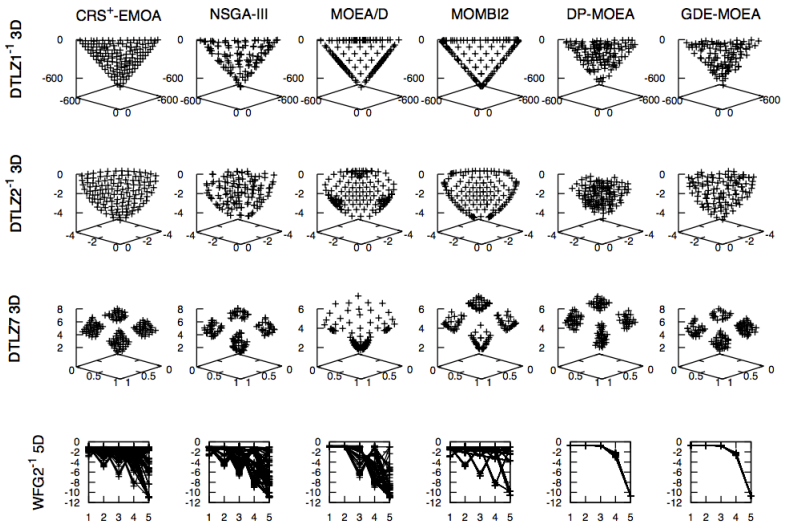

Fig. 2: Pareto fronts generated by CRS$^+$-EMOA and the adopted MOEAs. Each front corresponds to the median of the hypervolume value.

5 Conclusions and Future Work

Currently, most of the state-of-the-art MOEAs employ a set of convex weight vectors as search directions, reference set or as part of a quality indicator. This type of MOEAs have shown outstanding results on benchmark problems such as the DTLZ and WFG test suites. However, if these problems are slightly modified, then the performance of MOEAs based on convex weight vectors is significantly degraded. In this paper, we propose an Evolutionary Multi-Objective Algorithm based on the Combination of the Riesz s-energy and IGD$^+$ indicators that overcomes such overspecialization of state-of-the-art MOEAs on certain benchmark problems. Our proposed approach called CRS$^+$-EMOA, exploits the convergence property of IGD$^+$ and promotes evenly distributed solutions using s-energy. CRS$^+$-EMOA was compared with MOEAs using and not using convex weight vectors. The experimental results showed that our approach has a competitive performance on the DTLZ and WFG instances, while it outperforms the adopted MOEAs on the DTLZ^{-1} and WFG^{-1} problems. Based on the empirical results, we have an insight that CRS$^+$-EMOA is a more general multi-objective optimizer. As part of our future work, we are interested in improving the performance of CRS$^+$-EMOA on the original benchmark problems while preserving its good performance on the minus versions of the considered test suites. Another research direction that we want to explore is the combination of IGD$^+$ and s-energy in a single quality indicator.

References

1. Carlos A. Coello Coello, Gary B. Lamont, and David A. Van Veldhuizen. *Evolutionary Algorithms for Solving Multi-Objective Problems*. Springer, New York, second edition, September 2007. ISBN 978-0-387-33254-3.
2. Qingfu Zhang and Hui Li. MOEA/D: A Multiobjective Evolutionary Algorithm Based on Decomposition. *IEEE Transactions on Evolutionary Computation*, 11(6):712–731, December 2007.
3. Kalyanmoy Deb and Himanshu Jain. An Evolutionary Many-Objective Optimization Algorithm Using Reference-Point-Based Nondominated Sorting Approach, Part I: Solving Problems With Box Constraints. *IEEE Transactions on Evolutionary Computation*, 18(4):577–601, August 2014.
4. Raquel Hernández Gómez and Carlos A. Coello Coello. Improved Metaheuristic Based on the $R2$ Indicator for Many-Objective Optimization. In *2015 Genetic and Evolutionary Computation Conference (GECCO 2015)*, pages 679–686, Madrid, Spain, July 11-15 2015. ACM Press. ISBN 978-1-4503-3472-3.
5. Hisao Ishibuchi, Yu Setoguchi, Hiroyuki Masuda, and Yusuke Nojima. Performance of Decomposition-Based Many-Objective Algorithms Strongly Depends on Pareto Front Shapes. *IEEE Transactions on Evolutionary Computation*, 21(2):169–190, April 2017.
6. Kalyanmoy Deb, Samir Agrawal, Amrit Pratap, and T. Meyarivan. A Fast Elitist Non-Dominated Sorting Genetic Algorithm for Multi-Objective Optimization: NSGA-II. In Marc Schoenauer, Kalyanmoy Deb, Günter Rudolph, Xin Yao, Evelyne Lutton, Juan Julian Merelo, and Hans-Paul Schwefel, editors, *Proceedings of the Parallel Problem Solving from Nature VI Conference*, pages 849–858, Paris, France, 2000. Springer. Lecture Notes in Computer Science No. 1917.
7. Nicola Beume, Boris Naujoks, and Michael Emmerich. SMS-EMOA: Multiobjective selection based on dominated hypervolume. *European Journal of Operational Research*, 181(3):1653–1669, 16 September 2007.
8. Adriana Menchaca-Mendez and Carlos A. Coello Coello. GDE-MOEA : A New MOEA based on the Generational Distance indicator and ϵ-dominance. In *2015 IEEE Congress on Evolutionary Computation (CEC'2015)*, pages 947–955, Sendai, Japan, 25-28 May 2015. IEEE Press. ISBN 978-1-4799-7492-4.
9. Adriana Menchaca-Mendez, Carlos Hernández, and Carlos A. Coello Coello. Δ_p-MOEA: A New Multi-Objective Evolutionary Algorithm Based on the Δ_p Indicator. In *2016 IEEE Congress on Evolutionary Computation (CEC'2016)*, pages 3753–3760, Vancouver, Canada, 24-29 July 2016. IEEE Press. ISBN 978-1-5090-0623-9.
10. Hisao Ishibuchi, Hiroyuki Masuda, Yuki Tanigaki, and Yusuke Nojima. Modified Distance Calculation in Generational Distance and Inverted Generational Distance. In António Gaspar-Cunha, Carlos Henggeler Antunes, and Carlos Coello Coello, editors, *Evolutionary Multi-Criterion Optimization, 8th International Conference, EMO 2015*, pages 110–125. Springer. Lecture Notes in Computer Science Vol. 9019, Guimarães, Portugal, March 29 - April 1 2015.
11. D. P. Hardin and E. B. Saff. Discretizing Manifolds via Minimum Energy Points. *Notices of the AMS*, 51(10):1186–1194.
12. Hisao Ishibuchi, Noritaka Tsukamoto, Yuji Sakane, and Yusuke Nojima. Hypervolume Approximation Using Achievement Scalarizing Functions for Evolutionary Many-Objective Optimization. In *2009 IEEE Congress on Evolutionary Computation (CEC'2009)*, pages 530–537, Trondheim, Norway, May 2009. IEEE Press.

13. Simon Huband, Phil Hingston, Luigi Barone, and Lyndon While. A Review of Multiobjective Test Problems and a Scalable Test Problem Toolkit. *IEEE Transactions on Evolutionary Computation*, 10(5):477–506, October 2006.
14. Michael T.M. Emmerich, André H. Deutz, and Johannes W. Kruisselbrink. On Quality Indicators for Black-Box Level Set Approximation. In Emilia Tantar, Alexandru-Adrian Tantar, Pascal Bouvry, Pierre Del Moral, Pierrick Legrand, Carlos A. Coello Coello, and Oliver Schütze, editors, *EVOLVE - A bridge between Probability, Set Oriented Numerics and Evolutionary Computation*, chapter 4, pages 157–185. Springer-Verlag. Studies in Computational Intelligence Vol. 447, Heidelberg, Germany, 2013. 978-3-642-32725-4.